frontiers in Energy Research

ORIGINAL RESEARCH
published: 25 January 2017
doi: 10.3389/fenrg.2016.00041

Characteristics of Ti_3C_2X–Chitosan Films with Enhanced Mechanical Properties

Chunfeng Hu[1], Fei Shen[2], Degui Zhu[1], Haibin Zhang[3], Jianming Xue[4] and Xiaogang Han[2]**

[1] Key Laboratory of Advanced Technologies of Materials, Ministry of Education, School of Materials Science and Engineering, Southwest Jiaotong University, Chengdu, China, [2] Center of Nanomaterials for Renewable Energy, State Key Laboratory of Electrical Insulation and Power Equipment, School of Electrical Engineering, Xi'an Jiaotong University, Xi'an, China, [3] Institute of Nuclear Physics and Chemistry, China Academy of Engineering Physics, Mianyang, China, [4] State Key Laboratory of Nuclear Physics and Technology, Center for Applied Physics and Technology, Peking University, Beijing, China*

Chitosan-reinforced Ti_3C_2X films were successfully fabricated by infiltrating Ti_3C_2X suspensions containing different chitosan contents followed by vacuum drying. The designed chitosan contents were 0, 7, 10, and 14 wt%. It was determined that as-prepared films had shell-like nanolaminar microstructure. Displacement of Ti_3C_2X nanosheets increased from 24.254 Å (0 wt%) to 28.822 Å (10 wt%) and then decreased to 28.132 Å (14 wt%) with increment of chitosan content. Tensile strength of films continuously increased from 8.20 to 43.52 MPa, enhancing 5.3 times. Electrical resistivity of films increased from 0.39 mΩ cm (0 wt%) to 54.91 mΩ cm (14 wt%). Only pure Ti_3C_2X film could be used as electrode in the sodium battery.

Keywords: nanocomposites, microstructure, tensile strength, electrical resistivity, capacity

OPEN ACCESS

Edited by:
Hua Kun Liu,
University of Wollongong,
Australia

Reviewed by:
Manickam Minakshi,
Murdoch University, Australia
Caiyun Wang,
University of Wollongong,
Australia

****Correspondence:***
Chunfeng Hu
chfhu@live.cn;
Xiaogang Han
xiaogang.han@xjtu.edu.cn

Specialty section:
This article was submitted to Energy Storage, a section of the journal Frontiers in Energy Research

Received: *12 August 2016*
Accepted: *23 December 2016*
Published: *25 January 2017*

Citation:
Hu C, Shen F, Zhu D, Zhang H, Xue J and Han X (2017) Characteristics of Ti_3C_2X–Chitosan Films with Enhanced Mechanical Properties. Front. Energy Res. 4:41. doi: 10.3389/fenrg.2016.00041

INTRODUCTION

Nanolaminar $M_{n+1}X_n$ene (n=1–3) materials are new members of two-dimensional nanosheets, which were first discovered by Naguib et al. (2012). He dissolved Al element from MAX phases using high concentrated hydrofluoric acid (49 wt%) and got graphene-like carbides. These nanosheets exhibit excellent electrical conductivity and self-lubricity. To date, Ti_3C_2X, $(V_{0.5}Cr_{0.5})_3C_2X$, Mo_2TiC_2X, Cr_2TiC_2X, Ti_2CX, Nb_2CX, V_2CX, Mo_2CX, Nb_4C_3X, Ta_4C_3X, $Mo_2Ti_2C_3X$, $(Nb_{0.8}Ti_{0.2})_4C_3X$, and $(Nb_{0.8}Zr_{0.2})_4C_3X$ have been fabricated (Naguib et al., 2013; Ghidiu et al., 2014a; Sun et al., 2014; Anasori et al., 2015; Dall'Agnese et al., 2015; Meshkian et al., 2015; Yang et al., 2016). Here, X represents the functional groups of –OH, =O, and –F, which are formed during etching. Recently, Lukatskaya et al. systematically investigated the intercalation of ions into layered Ti_3C_2X in battery and electrochemical capacitor. She found that Na^+, K^+, NH_4^+, Mg^{2+}, and Al^{3+} ions could offer capacitance in excess of 300 F/cm^3, much higher than that of porous carbons (Lukatskaya et al., 2013). This study provided the evidence of electrochemical energy storage application of two-dimensional MXene using single and multivalent ions. Additionally, Ghidiu et al. (2014b) improved the volumetric capacitance up to 900 F/cm^3 with excellent cyclability and rate performance when using LiF/HCl solution etching Ti_3AlC_2 powder followed by rolling Ti_3C_2X clay as 5 μm thick film. This procedure provided the possibility of low cost production in industry. For other MXenes, the freestanding, flexible CNT/Nb_2CX paper electrodes were successfully prepared by Mashtalir et al. (2015) through filtering CNT/Nb_2CX suspension. More than 400 mAh/g of Li capacity at 0.5C and 325 F/cm^3 of volumetric capacitance tested in an Li-ion capacitor were achieved. As the lubricant, it was determined that Ti_3C_2X

nanosheets could effectively decrease the friction coefficient and enhance the wear resistance of countercouples of 440C stainless steel ball/45# steel disc as additive in 100 SN base oil (Zhang et al., 2015). The mechanism was attributed to sliding friction of nanosheets between the rubbing surfaces.

Recently, Ling et al. (2014) fabricated the Ti_3C_2X-PDDA/PVA polymer films and confirmed that as-obtained films showed high electrical conductivity of 2.24×10^4 S/m and high tensile strength of 30 MPa when the polymer loading was 10 wt%. As another important reinforcing polymer, chitosan has been widely used by combining graphene to prepare the composites applied in the fields of food industry, drug delivery, sensor, lithium-ion battery, and supercapacitor (Schiffman et al., 2009; Ramkumar and Minakshi, 2015). Chitosan, the N-deacetylated derivative of chitin, is commercially 85% deacetylated. Therefore, it is interesting to fabricate MXene–chitosan films and evaluate their physical and mechanical properties. In the present work, Ti_3C_2X–chitosan films were first prepared by colloidal method followed by vacuum infiltration. In order to systematically evaluate the physical and mechanical properties of as-obtained films, the microstructure, tensile strength, electrical resistivity, and capacity of sodium battery of films were investigated.

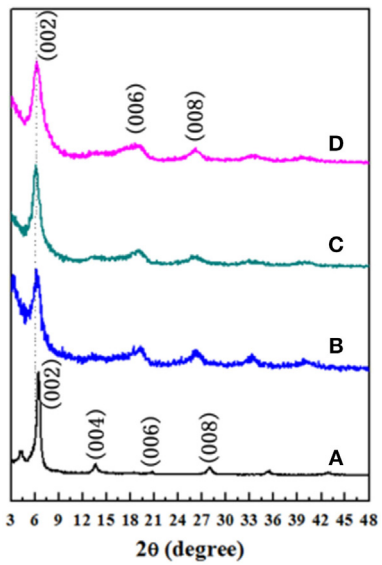

FIGURE 1 | X-ray diffraction patterns of Ti_3C_2X–chitosan films with different chitosan content: (A) 0, (B) 7, (C) 10, and (D) 14 wt%.

EXPERIMENTAL

Ti_3C_2X was prepared by immersing Ti_3AlC_2 powder into the solution of LiF/HCl for 40 h at 40°C followed by cleaning using deionized water until pH value of suspension reached 7. Then, the as-obtained suspension was ultrasonically stirred for 2 h at ambient temperature in a closed plastic bottle. After separating the Ti_3C_2X nanosheets through high-speed centrifugation (3,000 rpm) (ST16, Thermal Scientific, Inc., Odessa, TX, USA) for 10 min, the delaminated Ti_3C_2X could be well prepared by dispersing in the deionized water, showing a color of cyan. A total of 5 ml Ti_3C_2X suspension was filtered by vacuum filtration and dried in a vacuum chamber for 12 h. The concentration of suspension could be calculated according to the mass of Ti_3C_2X film, as 2.3 mg/ml. In order to prepare the Ti_3C_2X–chitosan films, first the chitosan from crab shells (molecular weight: 190,000–375,000 and DD: 83%) was weighed based on the designed content of 7, 10, and 14 wt%, and then mixed with 9 ml deionized water, 2 ml acetic acid (99.8 wt%), and 2 ml HCl (37 wt%). After oil bathing at 80°C for 5 min, the chitosan has been well dissolved in the solution. A total of 20 ml Ti_3C_2X suspension was poured into the chitosan solution and ultrasonically stirred for 10 min in order to get the homogeneous colloidal suspension. After vacuum filtering, as-prepared Ti_3C_2X–chitosan films were dried in the vacuum chamber for 12 h to remove the adsorbed water. For comparison, pure Ti_3C_2X film was also prepared.

The phase composition and microstructure of obtained films were characterized by an X-ray diffraction (XRD) diffractometer (SmartLab; Rigaku Corp., Tokyo, Japan) using CuKα radiation and a scanning electron microscope (Supra 50VP, Carl Zeiss AG, Germany) equipped with an energy dispersive spectroscope. The measurement of tensile strength was conducted by a KES G1 tensile tester (Kato Tech Co., Ltd., Kyoto, Japan) at a speed of 0.1 mm/s. For each composition, three to five specimens with a shape of dog bone were tested. The width of fracture region

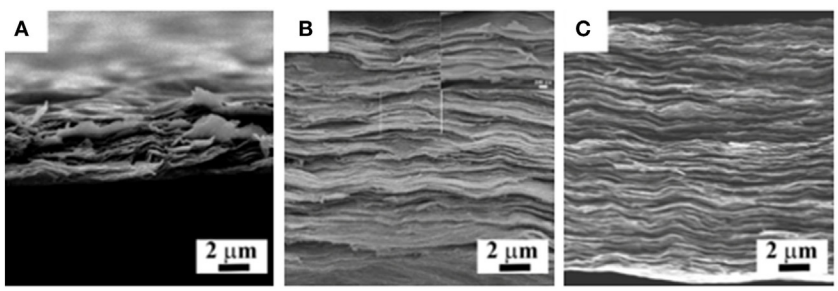

FIGURE 2 | Fracture surface of Ti_3C_2X–chitosan films after tensile testing: (A) 0, (B) 7, and (C) 14 wt%. (B) There is one magnified image of the rectangle region, showing delaminated layers.

was 2 mm. The electrical resistivity of films was tested by a four-probe facility (JANDEL, Jandel Engineering Ltd., Linslade, UK). 2032-type coin cell was fabricated to test the sodium ion storage performance. The as-prepared Ti_3C_2X film was punched to 10 mm disk and directly used as anode electrode, pure sodium metal used as the counter electrode, Celgard 2400 as separator and 1.0 M $NaPF_6$ in (1:1 V/V) ethylene carbonate/diethyl carbonate served as electrolyte. Galvanostatic cycling was conducted with a Land CT2001A tester at room temperature with potential window from 0.05 to 2 V vs Na/Na^+.

RESULTS AND DISCUSSION

Figure 1 shows XRD patterns of as-prepared Ti_3C_2X–chitosan films. It is seen that the main diffraction peak refers to (002) plane, which presents the preferential texture microstructure of films. Owing to its two-dimensional crystal structure, Ti_3C_2X nanosheets were prone to stack layer by layer during filtering. The long chains of chitosan covered the surface of nanosheets and were easy to lap with each other in the dried films. Here, there was an interesting phenomenon that after infiltration the initial thickness of Ti_3C_2X–chitosan films with water was about 5 mm and after drying the thickness of final film was only 14–16 μm, reducing more than 300 times. This reason might be attributed to the saturated adsorption of water among the Ti_3C_2X nanolayers, which inspires one good idea to prepare the aerogel of Ti_3C_2X in the following works. Additionally, it was found that during the drying process if there existed one hole less than 1 mm diameter in the film, it could completely disappear after drying, which exhibited a self-healing behavior. Probably, this material could be useful in the biological research. It was determined that the displacements between two Ti_3C_2X layers were 24.254, 27.384, 28.822, and 28.132 Å, respectively, for 0, 7, 10, and 14 wt% chitosan reinforced films (**Figures 1A–D**). The introduction of chitosan could expand the displacement of Ti_3C_2X nanosheets. When the content of chitosan was above 10 wt%, effect of more chitosan on the displacement became weak.

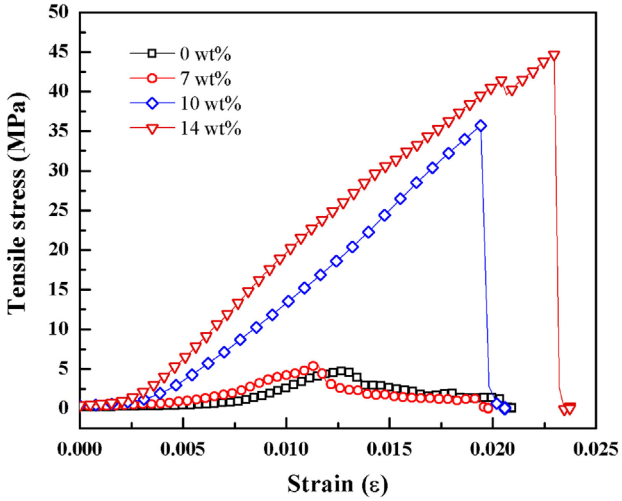

FIGURE 3 | Stress–strain curves of Ti_3C_2X–chitosan films.

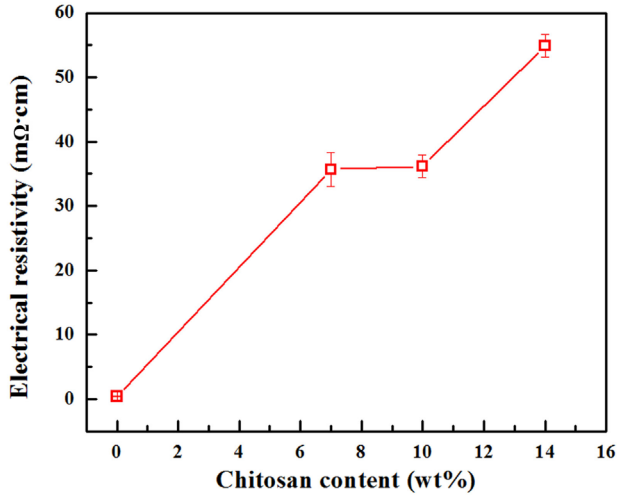

FIGURE 4 | Electrical resistivity of Ti_3C_2X–chitosan films as a function of chitosan content.

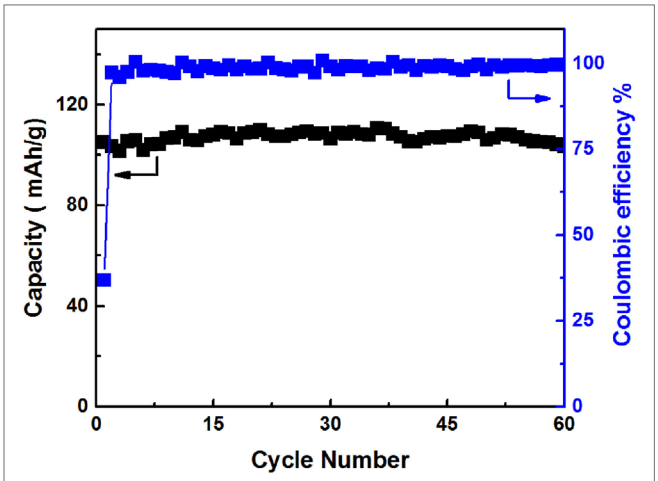

FIGURE 5 | Long-term electrochemical cycling of Ti_3C_2X–0 wt% chitosan film.

Figure 2 shows the fracture surface of Ti_3C_2X–chitosan films after tensile testing. It is observed that in the fracture surface of pure Ti_3C_2X film nanosheets arranged orderly and were torn and pulled out (**Figure 2A**). Some vacancies existed among the layers. Owing to the weak Van der Waals force, nanosheets were easily delaminated. The tensile strength was only 8.20 ± 4.63 MPa, as shown in **Figure 3**. When 7, 10, and 14 wt% chitosan were used as additives, the tensile strength could be increased up to 9.79 ± 5.31, 30.69 ± 5.01, and 43.52 ± 1.61 MPa continuously. At the same loading of 10 wt%, the tensile strength of Ti_3C_2X–chitosan films has a close value compared to that of Ti_3C_2X–PVA film (30 MPa) (Ling et al., 2014). By observing the fracture surface of Ti_3C_2X–7 wt% chitosan film, it is seen that the layers stacked more tightly in comparison with pure Ti_3C_2X film (**Figure 2B**). In the magnified image, the nanosheets were torn to be fractured

and spalling-off seldom appeared. Clearly, the chitosan has interacted with Ti_3C_2X nanosheets to form thin glue layers, acting as the intermedia to combine Ti_3C_2X nanosheets. However, some vacancies still existed in the fracture surface of film, which might be ascribed to the shortage of chitosan so that part surface of nanosheets could not be covered. Therefore, the tensile strength of film was only increased a few. When the chitosan content was designed above 10 wt%, especially as 14 wt%, nearly no vacancies could be observed in the fracture surface of film, as shown in **Figure 2C**. The morphology of film containing 10 wt% chitosan was similar to that of film with 14 wt% chitosan. So, the shell-like microstructure was successfully constructed and the as-obtained film with 14 wt% chitosan exhibited the highest tensile strength, about 5.3 times of that of pure Ti_3C_2X film. It is confirmed that 10 wt% chitosan is one critical value to strengthen the film. Whereas, in our works, more chitosan above 14 wt% could not be introduced into the film because the film was not possible to be prepared.

In addition, the electrical resistivity of as-prepared films was measured, as shown in **Figure 4**. With the increment of chitosan content, the film's resistivity increased gradiently. For pure Ti_3C_2X film, the measured electrical resistivity was 0.39 mΩ cm, as 2.56×10^5 S/m, which is close to the value determined by Ling et al. (2014) (2.4×10^5 S/m). Under the loading of 7 and 10 wt% chitosan, those of films were 35.69 and 36.21 mΩ cm, respectively. Also, the Ti_3C_2X–14 wt% chitosan film exhibited electrical resistivity of 54.91 mΩ cm. So, it is reasonable to believe that the optimized chitosan content is 10–14 wt% to design Ti_3C_2X–chitosan films with excellent mechanical properties.

The sodium ion storage property of Ti_3C_2X–chitosan films was further performed. As shown in **Figure 5**, a revisable capacity above 100 mAh/g is obtained with Coulombic efficiency nearly to 100% during cycling. However, it was found that when the film contained chitosan, the sodium ion storage capacity dropped sharply. The reason might be that the introduction of chitosan might block electrolyte transport pathways within Ti_3C_2X flakes and decrease the electrical conductivity of electrodes as well.

CONCLUSION

Nanolaminar Ti_3C_2X–chitosan films were well prepared with the polymer loading of 0, 7, 10, and 14 wt%. It was found that these films exhibited the shell-like microstructure. With the increasing content of chitosan, the displacement between Ti_3C_2X nanosheets increased from 24.254 Å (0 wt%) to 28.822 Å (10 wt%) and then decreased to 28.132 Å (14 wt%). The tensile strength of films continuously increased from 8.20 to 43.52 MPa, enhancing 5.3 times. Additionally, the electrical resistivity of films increased from 0.39 (0 wt%) to 54.91 mΩ cm (14 wt%). Only pure Ti_3C_2X film could be used as electrode in the sodium battery.

AUTHOR CONTRIBUTIONS

XH and CH provided the idea and organized the manuscript. DZ, HZ, JX, and FS contributed to the experiments and characterization, and also discussed the results.

ACKNOWLEDGMENTS

This work is supported by "ChuYing" Program of Southwest Jiaotong University, Thousand Talents Program of Sichuan province, and National Natural Science Foundation of China (U1232136, 91226202, 51521065). The authors thank the suggestions of Dr. Michel Barsoum in Drexel University.

REFERENCES

Anasori, B., Xie, Y., Beidaghi, M., Lu, J., Hosler, B. C., Hultman, L., et al. (2015). Two-dimensional, ordered, double transition metals carbides (MXenes). *ACS Nano* 9, 9507–9516. doi:10.1021/acsnano.5b03591

Dall'Agnese, Y., Taberna, P. L., Gogotsi, Y., and Simon, P. (2015). Two-dimensional vanadium carbide (MXene) as positive electrode for sodium-ion capacitors. *J. Phys. Chem. Lett.* 6, 2305–2309. doi:10.1021/acs.jpclett.5b00868

Ghidiu, M., Naguib, M., Shi, C., Mashtalir, O., Pan, L. M., Zhang, B., et al. (2014a). Synthesis and characterization of two-dimensional Nb_4C_3 (MXene). *Chem. Commun.* 50, 9517–9520. doi:10.1039/C4CC03366C

Ghidiu, M., Lukatskaya, M. R., Zhao, M. Q., Gogotsi, Y., and Barsoum, M. W. (2014b). Conductive two-dimensional titanium carbide clay with high volumetric capacitance. *Nature* 516, 78–81. doi:10.1038/nature13970

Ling, Z., Ren, C. E., Zhao, M. Q., Yang, J., Giammarco, J. M., Qiu, J. S., et al. (2014). Flexible and conductive MXene films and nanocomposites with high capacitance. *Proc. Natl. Acad. Sci. U.S.A.* 111, 16676–16681. doi:10.1073/pnas.1414215111

Lukatskaya, M. R., Mashtalir, O., Ren, C. E., Dall'Agnese, Y., Rozier, P., Taberna, P. L., et al. (2013). Cation intercalation and high volumetric capacitance of two-dimensional titanium carbide. *Science* 341, 1502–1505. doi:10.1126/science.1241488

Mashtalir, O., Lukatskaya, M. R., Zhao, M. Q., Barsoum, M. W., and Gogotsi, Y. (2015). Amine-assisted delamination of Nb_2C MXene for Li-ion energy storage devices. *Adv. Mater. Weinheim* 27, 3501–3506. doi:10.1002/adma.201500604

Meshkian, R., Näslund, L. Å, Halim, J., Lu, J., Barsoum, M. W., and Rosen, J. (2015). Synthesis of two-dimensional molybdenum carbide, Mo_2C, from the gallium based atomic laminate Mo_2Ga_2C. *Scr. Mater.* 108, 147–150. doi:10.1016/j.scriptamat.2015.07.003

Naguib, M., Come, J., Dyatkin, B., Presser, V., Taberna, P. L., Simon, P., et al. (2012). MXene: a promising transition metal carbide anode for lithium-ion batteries. *Electrochem. Commun.* 16, 61–64. doi:10.1016/j.elecom.2012.01.002

Naguib, M., Halim, J., Lu, J., Cook, K. M., Hultman, L., Gogotsi, Y., et al. (2013). New two-dimensional niobium and vanadium carbides as promising materials for Li-ion batteries. *J. Am. Chem. Soc.* 135, 15966–15969. doi:10.1021/ja405735d

Ramkumar, R., and Minakshi, M. (2015). Fabrication of ultrathin $CoMoO_4$ nanosheets modified with chitosan and their improved performance in energy storage device. *Dalton Trans.* 44, 6158–6168. doi:10.1039/C5DT00622H

Schiffman, J. D., Stulga, L. A., and Schauer, C. L. (2009). Chitin and chitosan: transformations due to the electrospinning process. *Polymer Eng. Sci.* 49, 1918–1928. doi:10.1002/pen.21434

Sun, D. D., Wang, M. S., Li, Z. Y., Fan, G. X., Fan, L. Z., and Zhou, A. G. (2014). Two-dimensional Ti_3C_2 as anode material for Li-ion batteries. *Electrochem. Commun.* 47, 80–83. doi:10.1016/j.elecom.2014.07.026

Yang, J., Naguib, M., Ghidiu, M., Pan, L. M., Gu, J., Nanda, J., et al. (2016). Two-dimensional Nb-based M_4C_3 solid solutions (MXenes). *J. Am. Ceramic Soc.* 99, 660–666. doi:10.1111/jace.13922

Zhang, X. H., Xue, M. Q., Yang, X. H., Wang, Z. P., Luo, G. S., Huang, Z. D., et al. (2015). Preparation and tribological properties of $Ti_3C_2(OH)_2$ nanosheets as additives in base oil. *RSC Adv.* 5, 2762–2767. doi:10.1039/C4RA13800G

Conflict of Interest Statement: The authors declare that the research was conducted in the absence of any commercial or financial relationships that could be construed as a potential conflict of interest.

The reviewer CW and handling editor declared their shared affiliation, and the handling editor states that the process nevertheless met the standards of a fair and objective review.